Trajectory Optimization for Variable-Density Spiral Two-Dimensional Excitation

Y. S. Levin[1,2], L. J. Pisani[1], D. M. Spielman[1,2], J. M. Pauly[2]

[1]Department of Radiology, Stanford University School of Medicine, Stanford, CA, United States, [2]Department of Electrical Engineering, Stanford University School of Engineering, Stanford, CA, United States

Introduction Two-dimensional excitation pulses have found numerous uses in MR imaging. Variable-density (VD) 2-D spiral excitation has been investigated as a way to shorten the duration of excitation pulses, limit RF power deposition, and "spread out" sidelobes (1,2). Tikhonov regularization has recently been used to further optimize the RF pulse for a given VD spiral trajectory (3). However, to our knowledge, no published work optimizes the actual trajectory in excitation k-space, i.e. the gradient waveform. This work proposes a simple method to accomplish this task.

Theory The algorithm optimizes the excitation k-space trajectory for variable-density spirals by approximating the trajectory by concentric circles. This same approximation was used by Pauly, et al in describing linear large tip-angle pulses. Pauly showed that for an rf-weighted trajectory in excitation k-space that is hermitian symmetric, the fourier transform of the weighted trajectory is the flip angle (in radians) as a function of position (4). Because a circle is radially symmetric, its Fourier transform is also radially symmetric and can be expressed one-dimensionally as the Hankel transform: $\delta(k_r\text{-}k_{r0}) \longleftrightarrow (2\pi k_{r0})\, J_0(2\pi k_{r0} r)$, where $J_0(\bullet)$ refers to the zeroth-order Bessel function of the first kind (5). Thus, the flip angle can be approximated as $\theta(r) = \Sigma^{N}_{i=1}\ (\gamma B_{1i})(\ k_{ri}\ ) J_0(2\pi k_{ri} r)$ where N is the total number of circles and B_{1i} are chosen to achieve the desired k-space weighting for a 180° flip after appropriate density compensation. The slice profile, P(r), is simply $cos(\theta(r))$ and $sin(\theta(r))$ for inversion and excitation, respectively.

Procedure The "circle approximation" was used to design an inversion pulse with a width of 1 cm. Nominal field of view was chosen to be 10 cm. Thus, the uniform-density trajectory is a series of equally spaced rings with radii in excitation k-space extending from $k_r = .1\ cm^{-1}$ to $k_r = 1\ cm^{-1}$ in steps of $.1\ cm^{-1}$, expressed in vector form as $\mathbf{k}$ = [.1 .2 .3 .4 .5 .6 .7 .8 .9 1]. Variable density trajectories, described by the vector $\mathbf{k_v}$, were derived from $\mathbf{k}$ as a polynomial: $\mathbf{k_v} = (c_1\mathbf{k} + c_2\mathbf{k}.^2 + c_3\mathbf{k}.^3 + c_4\mathbf{k}.^4)/(\max\|c_1\mathbf{k} + c_2\mathbf{k}.^2 + c_3\mathbf{k}.^3 + c_4\mathbf{k}.^4\|)$, where the fourth-order vector refers to element-by-element exponentiation and the denominator normalizes the vector describing the radii of the circles so that the maximum is at $k_r = 1\ cm^{-1}$. A global search was performed for all values of c_i from 0 to 1 in steps of 0.1. The maximum sidelobe height for each trajectory was recorded, and the polynomial coefficients yielding the minimum value over all trajectories was used in designing the pulse. The polynomial search was limited to fourth order to avoid lengthy computation times; the improvement in going from third order to fourth order was small, and a fifth-order term did not seem likely to provide further improvement. In order to test the accuracy of the circle approximation, the forward SLR transform was performed for each of the corresponding spiral trajectories, and the maximum sidelobe height was recorded and compared to the value obtained from the circle approximation.

Results Search speed for the circle approximation exceeded that of the SLR transform by a factor of 16 (25 minutes vs. 6.75 hrs using MATLAB 6.5 and an Intel Pentium 4 2.26 GHz processor). The "optimal" set of coefficients c_i was found to be [1 0 0 .4]. Figure 1 depicts the slice profile for the corresponding "circle" trajectory (blue) and spiral trajectory (red). The sidelobes do not completely coincide for the two trajectories because of the anti-symmetric nature of sampling for the spiral trajectory. However, the peak sidelobe height is comparable. Figure 2 depicts a scatterplot of peak sidelobe height for the spiral trajectory versus the circular trajectory for all of the trajectories sampled. Although the circle approximation does not precisely correspond to the spiral approximation, there is a close correlation. Furthermore, the optimal circle trajectory is also optimal for the spiral trajectory. Figure 3 depicts a cut through the two-dimensional inversion profile (computed using a numerical solution of the Bloch equation) for the uniform density (blue) and optimized variable density (red) spiral. For the uniform density spiral, the peak sidelobe height is 5% of the mainlobe height; the variable density spiral, the peak sidelobe is only 1% of the mainlobe height. Figure 4 depicts the trajectory in excitation k-space (4a) and the shapes of the rf waveforms (4b) for the uniform density (blue) and variable density (red) spirals.

Figure 1

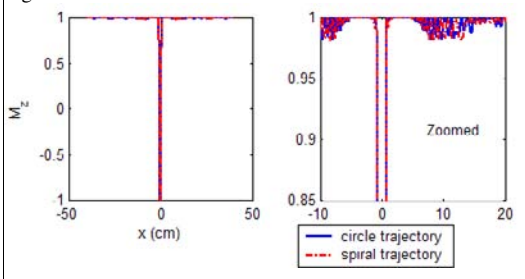

Figure 2

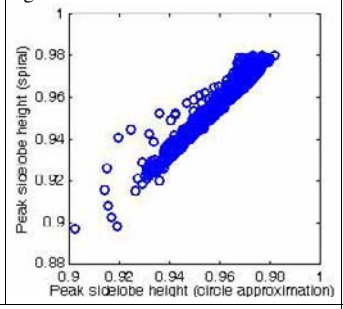

Figure 3

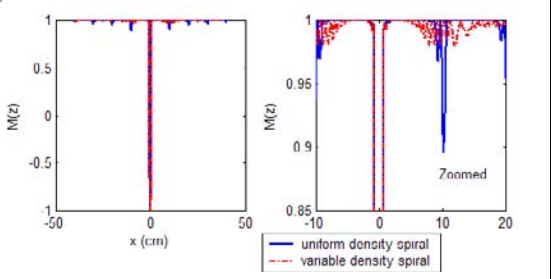

Figure 4a

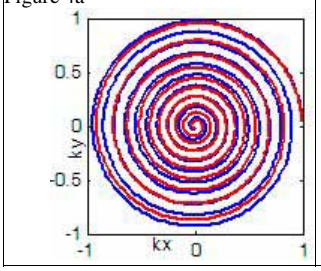

Figure 4b

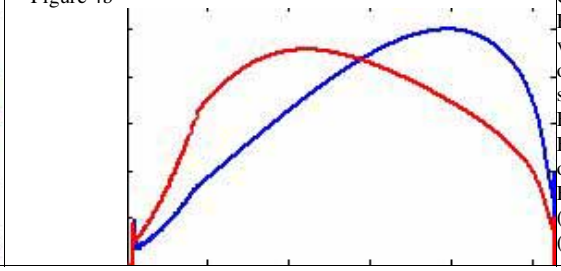

Captions:
Figure 1: Comparison of slice profile obtained using the optimized variable-density circle approximation (blue) with slice profile obtained using the forward SLR transform on the corresponding spiral trajectory (red).
Figure 2: Spiral vs. Circle approximation: Peak sidelobe height.
Figure 3: Slice profile for uniform density spiral (blue) and optimized variable density spiral (red).
Figure 4: Trajectory in excitation k-space (4a) and RF waveform (4b) for uniform-density (blue) and optimized variable density (red) spirals.

Conclusions: The "circle approximation" allows for fast and accurate optimization of the excitation k-space trajectory, with an 80% reduction in peak sidelobe height for the 1-cm inversion pulse investigated here. This significant reduction in peak sidelobe height likely makes it possible to allow the sidelobe to alias inside the field of view. If the 1% peak sidelobe height can be tolerated, the FOV constraint present in the design of uniform density spirals can be eliminated. Thus, the 1 cm variable density inversion pulse described here can be implemented in arterial spin labeling in a volume that is much larger than the nominal 10 cm FOV. The application to excitation pulses is straightforward, although the sidelobe reduction will not be as great for such a pulse because the slice profile is $\sin(\theta) \sim \theta$, rather than $\cos(\theta) \sim 1\text{-}\theta^2$ for the inversion pulse.

References: (1) Schroder et al. JMRI 2003;18:136-141. (2) Stenger et al. MRM 2003;50:1100-1106 (3) Yip et al. MRM 2005;54:908-917. (4) Pauly et al. JMR 1989;82:571-587. (5) Bracewell. The Fourier Transform and its Applications. Second Edition, McGraw-Hill 1986.